Acta Cryst. (1993). B49, 655–661

Lattice Modulation of the ε-Phase in a Cu–Sb Alloy

BY KUMI MOTAI AND YOUSUKE WATANABE

Institute for Materials Research, Tohoku University, Katahira 2-1-1, *Aobaku, Sendai* 980, *Japan*

AND SHINYA HASHIMOTO

Japan Institute of Atomic Energy, Tokai Branch, Tokai, Ibaraki 319-11, *Japan*

(*Received* 30 *August* 1991; *accepted* 25 *March* 1993)

Abstract

The ε-phase in a Cu–Sb binary alloy (19.5 at.% Sb), which is characterized by a two-dimensionally modulated structure, has been investigated by single-crystal X-ray diffraction at ambient temperature (290 K). The structure analysis was performed based on a five-dimensional superspace group $P^{P6_3/mmc}_{p6\ 1\,mm}$ using occupational and displacive modulation waves. The final agreement factors are $R_0 = 0.086$ and $R_1 = 0.128$ for 54 basic reflections and 75 first-order satellites, respectively. Very weak second-order satellites of $\mathbf{k}_1 + \mathbf{k}_2$ type are observed using Cu $K\alpha$ radiation, but the other type of second-order satellites are too weak to detect in the present investigation. The analysis indicates that mixed occupation of Cu and Sb occurs extensively, contrary to the model from a high-resolution electron microscopy study. With regard to the atomic displacements, the transverse component is larger than the longitudinal component, which is in contrast to the Au–Cd alloy. Crystal data of the basic structure: $M_r = 74.90$, hexagonal, $P6_3/mmc$, $a = 2.737\ (4)$, $c = 4.320\ (2)$ Å, $V = 28.03\ (6)$ Å^3, $Z = 2$, $D_x = 8.88$ Mg m^{-3}, λ(Mo $K\alpha$) = 0.7107 Å, μ(Mo $K\alpha$) = 39.2 mm^{-1}, $F(000) = 66.6$, two-dimensional wavevectors $\mathbf{k}_1 = 0.430\ (1)(\mathbf{b}_1 + \mathbf{b}_2)$, $\mathbf{k}_2 = 0.430\ (1)(-\mathbf{b}_1 + 2\mathbf{b}_2)$.

Introduction

The study of the crystal structure of the ε-phase which occurs in Cu–Sb alloys near 20 at.% Sb has a long history (Hansen, 1958). By application of single-crystal X-ray diffraction methods, Gunzel & Schubert (1958) obtained first-order satellites and estimated the structure to be a superstructure with an Mg_3Cd-type (DO19) ordered lattice. Yamaguchi & Hirabayashi (1972) studied the structure in more detail and suggested a model similar to the superstructure they had determined in Au–Cd alloys near 30 at.% Cd (Hirabayashi *et al.*, 1970). With respect to the positions of the first-order satellites, the diffraction pattern is the same as those of the Au–Cd alloys. The essential difference, however, is that the ε-phase of the Cu–Sb alloy is intrinsically incommensurate and there is no composition which gives the commensurate structure, in contrast to the Au–Cd alloys.

At that time, there was no established way of analysing incommensurate structures by diffraction methods. However, Hirabayashi, Hiraga & Shindo (1981) solved the incommensurate structure of Au–Cd alloys by application of high-resolution electron-microscopy techniques. The same method was also applied by Onozuka, Kakehashi, Takahashi & Hirabayashi (1989) for the Cu–Sb alloys discussed here. They reported that the crystal structure of the ε-phase (19.1% Sb) alloy can be described as commensurate containing 3456 atoms and having hexagonal lattice parameters $a = 24(3^{1/2})a_0$ and $c = c_0$, where a_0 and c_0 are parameters corresponding to the disordered hexagonal lattice.

Meanwhile, structure analysis by diffraction methods using higher dimensional symmetry has been established and widely applied to the X-ray diffraction data for various incommensurately modulated crystals (Janssen & Janner, 1987; Steurer, 1989). The direct observation of the real lattice using high-resolution electron microscopy seems to be more powerful than the indirect diffraction methods. However, in the case of modulated structures, the modulation is almost always accompanied by atomic displacement in addition to atomic concentration. This atomic displacement can be as small as 0.01 Å and is difficult to detect by electron microscopy. The significance of this atomic displacement was studied theoretically by Kataoka & Iwasaki (1981). Watanabe & Iwasaki (1982) showed this small atomic displacement wave in Au–33 at.% Cd using X-ray diffraction and conventional methods of analysis. Yamamoto (1983) later showed the usefulness of five-dimensional analysis when applied to the Au–Cd alloy, using data obtained from the above authors.

Therefore, there are two important problems relating to the structure of ε-phase that remain: the

first is whether the incommensurate structure can really be explained by considering a giant cell, as discussed by Onozuka *et al.* (1989); the second is to clarify the structure by applying X-ray diffraction and higher dimensional symmetry analysis, and also to highlight differences between this structure and that of Au–Cd.

Experimental procedures

Several alloy ingots of composition near to 19 at.% Sb were first prepared by melting Cu (99.999% pure) and Sb (99.99% pure) in an evacuated quartz capsule. Small chips cut from the ingots were melted again in a capsule at 993 K, cooled down to 623 K and then annealed for one month to attain an equilibrium state of the ε-phase. As expected from the complex phase diagram of this alloy (Hansen, 1958), it was very difficult to grow large single crystals. Most of the chips were polycrystalline, but very occasionally a single-crystal chip with chemical composition of 19.5 at.% Sb was obtained from the ingot by deep etching in an aqueous solution of hydrofluoric and nitric acids. The size of the crystal selected for the diffraction studies was 0.02 × 0.05 × 0.15 mm and it had a complicated shape like a truncated ellipsoid. No absorption correction was applied. The general features of the reciprocal lattice were examined using a precession camera. The basic lattice has a hexagonal symmetry and the satellites take an incommensurate position of the basic lattice giving $M = 7.19\,(0.01)$, the definition of which is given in Fig. 1.*

* The definition of M corresponds to $2M$ in the paper of Onozuka *et al.* (1989).

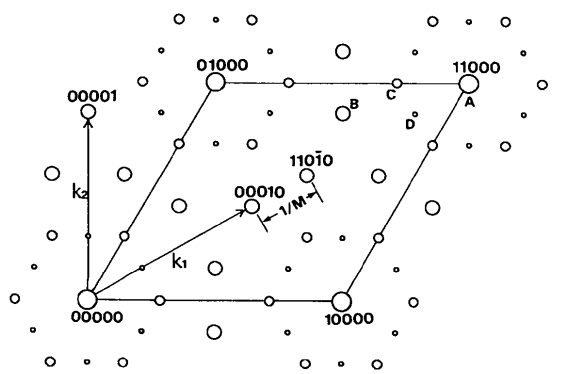

Fig. 1. Directions of the two modulation vectors, $\mathbf{k}_1$ and $\mathbf{k}_2$ in the reciprocal lattice and the definition of M which corresponds to the period of the superstructure. The largest circles, A, at the corner of the parallelogram indicate the main or basic reflections; the next-largest circles, B, indicate first-order satellites; the intermediate circles, C, indicate second-order satellites of $\mathbf{k}_1 + \mathbf{k}_2$ type; and the smallest circles, D, indicate second-order satellites of $2\mathbf{k}_1$ or $2\mathbf{k}_2$ type.

The X-ray diffraction experiments were carried out using a Rigaku AFC-6 diffractometer. Measurements of the basic lattice reflections were performed using Mo $K\alpha$ radiation monochromated with 002 reflection from pyrolytic graphite. For measurements of the incommensurate satellites, a Huber Eulerian cradle (type 511) was used in conjunction with a goniometer (type 422).

The crystal quality was examined and found to be poor, and the diffraction profiles changed depending on the indices and scanning directions. One example is given in Fig. 2 which shows asymmetry and small splitting. The profiles of the main reflections are much better than those of the satellites. The first-order satellites were measured using Mo $K\alpha$ radiation and a graphite monochromator. Very weak reflections of the second and higher orders were measured using Cu $K\alpha$ radiation. It was found that Cu $K\alpha$ radiation was preferable to Mo $K\alpha$ radiation in detecting very weak reflections. A comparison of the two types of radiation is shown in Fig. 3. The substitution of air by He gas was tested using Mo $K\alpha$ radiation, but the improvement of signal-to-noise ratio was poor in comparison to Cu $K\alpha$ radiation. However, the use of Cu $K\alpha$ radiation has two

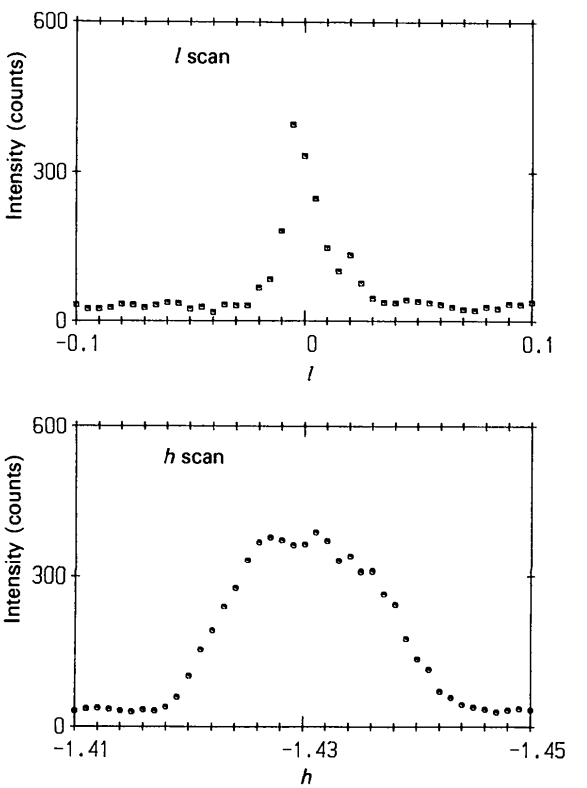

Fig. 2. Difference of the profiles along **a*** (bottom) and **c*** (top). The reflection is $\bar{1}10\bar{1}0$ or $\overline{1.43}0.570$. Cu $K\alpha$ radiation, 40 kV × 30 mA, counting time 40 s for each point.

serious drawbacks, *i.e.* lack of quantitativeness in the intensity due to high X-ray absorption and considerable reduction in the observable range in reciprocal space as a result of the longer wavelength. It should be mentioned that the observable limit is not solely determined by the radius of the Ewald sphere but also by the design of the goniometer. For the present apparatus with off-center type cradle, the maximum accessible angular range in ω for any χ is only 31° and beyond this angle the collimator collides with the χ-circle. A total of 21 satellites were measured in the reciprocal-lattice unit nearest to the origin: nine for the second order of $\mathbf{k}_1 + \mathbf{k}_2$ type, six for the second order of $2\mathbf{k}_1$ or $2\mathbf{k}_2$ type, and the remaining six which should have observable intensities if the structure model of Onozuka is appropriate. (See the definition of the types of second-order satellites in Fig. 1.) Data-collection conditions are summarized in Table 1.

Table 1. *Summary of experimental conditions*

No. of reflections for lattice parameters	14 ($36 > 2\theta > 17°$)
Standard reflections	3 (variation within 2%)
Measured reflections	
Basic structure (Mo $K\alpha$)	865 (662, $\|F_o\| > 3\sigma$)
No. of independent reflections	54
R_{int}	0.084
Range of h, k, l	$\|h\|, \|k\| \le 4, \|l\| \le 8$
Satellites	
First order (Mo $K\alpha$)	540 (434, $\|F_o\| > 3\sigma$)
No. of independent reflections	75
R_{int}	0.146
Range of h, k, l	$\|h\|, \|k\| \le 4, \|l\| \le 6$
No. higher than first order (Cu $K\alpha$)	21
Range of h, k, l	$h < 2, k < 1, l \le 1$
Data-collection mode	
Basic structure	$2\theta < 30°$, ω scan; $2\theta \ge 30°$, ω–2θ scan
Scan speed (° min $^{-1}$)	1
Scan width	$\Delta\omega = (3.5 + 0.5\tan\theta)°$ (Mo $K\alpha$)
Modulated structure	ω-step scan with interval $\Delta\omega = 0.2°$
Counting time for each step (s)	4, 10, 20, 100, 200 (depending on intensity)
Scan width	$\Delta\omega = (3.0 + 0.6\tan\theta)°$ (Mo $K\alpha$) $\Delta\omega = (3.0 + 0.3\tan\theta)°$ (Cu $K\alpha$)

Structure determination

A reflection condition found in the observed intensity data, $hh\bar{2}\bar{h}l$: $l = 2n$, indicates that a possible space group for the basic structure is $P6_3/mmc$ only if we allow the presence of inversion symmetry. Another reflection condition, if $h - k = 3n$ then $l = 2n$, indicates that the possible atomic positions are 2(*c*) or 2(*d*), using the Wyckoff notation, if the basic hexagonal unit cell contains two atoms. We chose the 2(*c*) site. Thus the basic (or averaged) structure has the same symmetry as that of Au–Cd (Watanabe & Iwasaki, 1982). As described earlier, the positions of the first-order satellites are the same as those of the Au–Cd alloy. Thus, we can use the same two-dimensional modulation wavevectors, as shown in Fig. 1, where the indices are expressed using five-index notation, $\mathbf{h} = h_1\mathbf{b}_1 + h_2\mathbf{b}_2 + h_3\mathbf{b}_3 + h_4\mathbf{k}_1 + h_5\mathbf{k}_2$, where $\mathbf{k}_1 = [\frac{1}{2} - 1/(2M)](\mathbf{b}_1 + \mathbf{b}_2)$ and $\mathbf{k}_2 = [\frac{1}{2} - 1/(2M)](-\mathbf{b}_1 + 2\mathbf{b}_2)$. Contrary to the case of the Au–Cd alloy, in which the observable satellites were limited only to the first order, second-order satellites could also be observed in the present Cu–Sb alloy as shown in Fig. 3. There are two possible types of second-order satellites: one is the sum of the same kind of first-order satellites, $2\mathbf{k}_1$ or $2\mathbf{k}_2$, and the other is the sum of different kinds, $\mathbf{k}_1 + \mathbf{k}_2$ (*D* and *C* in Fig. 1, shown by the smallest and next-to-smallest circles, respectively). The former type was rarely observed in the diffraction patterns of the present alloy. This may be due to an antiphase domain structure in the alloy. Fig. 4 shows the two pairs of first-order satellites (*A*1 and *B*1 or *A*2 and *B*2) which correspond to splitting of the superlattice reflections in ordered alloys having antiphase domain structure (Okamura, Iwasaki & Ogawa, 1968). By comparing the two pairs, it is clear that the ratio of intensity of the pair increases with h, *i.e.* $A1/B1 > 1$ and $A2/B2 \gg 1$. This indicates the existence of a relatively large atomic displacement modulation, in addition to the occupational modulation. It is interesting that the sense of the intensity ratio is opposite to that of the Au–Cd alloy, *i.e.* $A/B < 1$ [refer to A and B or <u>A</u> and <u>B</u> in Fig. 2 of Watanabe & Iwasaki (1982)]. The reflection condition, $h_1h_1h_3h_40$: $h_3 = 2n$, indicates that the symmetry operation $(S_3|0,0,\frac{1}{2},0,0)$ exists, and that the Bravais lattice is $P6/mmm(\alpha\alpha0)$ (Janner, Janssen & Wolff, 1983). The space group is $P^{P6_3/mmc}_{p6\ 1\ mm}$ which is identical to that of the Au–Cd alloy (Yamamoto, 1983; Budkowski, Marinkovic, Prodan & Boswell, 1990).

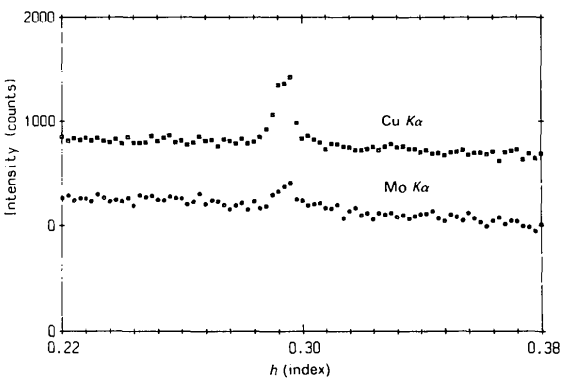

Fig. 3. Comparison of the reflection profiles of the second-order satellite $\bar{1}012\bar{1}$ or 0.2901 for Cu $K\alpha$ and Mo $K\alpha$ radiation: 40 kV × 30 mA, counting time 200 s for each point. The intensity scale is common to both radiation types and the shift of the origin serves to distinguish between them.

We next determine the forms of the occupational and displacive modulation waves up to the observable second order of $k_1 + k_2$ type that are allowed by

the above symmetry. The final result for the displacement wave is given as follows:

$$\begin{aligned}\mathbf{u}(x_4,x_5) = U_1\{&-(\mathbf{a}+\mathbf{b})\sin 2\pi x_4 - \mathbf{b}\sin 2\pi x_5 \\ &- \mathbf{a}\sin[2\pi(x_4-x_5)]\} \\ &+ U_2\{(-\mathbf{a}+\mathbf{b})\cos 2\pi x_4 \\ &+ (2\mathbf{a}+\mathbf{b})\cos 2\pi x_5 \\ &- (\mathbf{a}+2\mathbf{b})\cos[2\pi(x_4-x_5)]\} \\ &+ U_3\{(\mathbf{a}+2\mathbf{b})\sin[2\pi(x_4+x_5)] \\ &+ (2\mathbf{a}+\mathbf{b})\sin[2\pi(2x_4-x_5)] \\ &+ (-\mathbf{a}+\mathbf{b})\sin[2\pi(-x_4+2x_5)]\} \\ &+ U_4\{-(\mathbf{a}+2\mathbf{b})\cos[2\pi(x_4+x_5)] \\ &+ (2\mathbf{a}+\mathbf{b})\cos[2\pi(2x_4-x_5)] \\ &+ (-\mathbf{a}+\mathbf{b})\cos[2\pi(-x_4+2x_5)]\}, \qquad (1)\end{aligned}$$

where **a** and **b** are the primitive translational vectors of the basal plane in the hexagonal lattice, and U_1 and U_2 are parameters corresponding to the first-order triple waves of longitudinal and transverse types, respectively. U_3 and U_4 correspond to second-order waves of $\mathbf{k}_1+\mathbf{k}_2$ type. x_4 and x_5 are the coordinates in hyperspace, with $x_4=[\frac{1}{2}-1/(2M)](x_1+x_2)$ and $x_5=[\frac{1}{2}-1/(2M)](-x_1+2x_2)$, where x_1 and x_2 are the coordinates in the three-dimensional space. The first-order terms have amplitudes of U_1 and U_2 given by Yamamoto (1983) and the longitudinal U_1 component given by Watanabe & Iwasaki (1982).

A similar expression for the occupational waves is given as,

$$\begin{aligned}P(x_4,x_5) = P_0 &+ P_1[\cos 2\pi x_4 + \cos 2\pi x_5 + \cos 2\pi(x_4-x_5)] \\ &+ P_2[\sin 2\pi(2x_4-x_5) - \sin 2\pi(x_4+x_5) \\ &+ \sin 2\pi(-x_4+2x_5)] \\ &+ P_3[\cos 2\pi(2x_4-x_5) \\ &+ \cos 2\pi(x_4+x_5) + \cos 2\pi(-x_4+2x_5)], \qquad (2)\end{aligned}$$

where P_0 is the average concentration of copper and is given according to the chemical composition as 0.805, P_1 is the first-order parameter, and P_2 and P_3 are the second-order parameters of the triple waves. The first two terms having amplitude P_0 and P_1 are the same as those of Watanabe & Iwasaki (1982) and Yamamoto (1983). The isotropic temperature factor has the same form as in (2). Thus the number of parameters is eleven in all: four for displacement waves, three for occupational waves and four for temperature factors.

A least-squares fitting program for multidimensional space analysis (*REMOS*), written by Yamamoto, was used for the structure refinement with respect to $|F_o|$ using (1) and (2). Unit weights were used. Atomic scattering factors and anomalous-dispersion correction factors were taken from *International Tables for X-ray Crystallography* (1974, Vol. IV, pp. 79, 85, 99, 149). In the course of the least-squares calculations, the second-order parameters were determined separately because there were only nine second-order reflections.

The final R values for basic, first- and second-order reflections were 0.086, 0.128 and 0.449, respectively, and the resultant parameters are given in Table 2.* The ratio of maximum shift to e.s.d., $(\Delta/\sigma)_{max}$, was 0.02 in the last cycle. The final parameters and R value for the second-order satellites only have qualitative significance (see Tables 2 and 3), and it is worthwhile examining how the final parameters are affected by adding reflections which are beyond the observable limit. Since intensities of the second-order reflections are very weak, they may be approximated to zero or 'vanished'. By adding 21 'vanished' second-order reflections to the nine observed reflections in the least-squares refinement, the final analysis indicates that the values of U_3 and U_4 are altered significantly, giving much smaller values of -0.0001 and 0.0013, respectively, in comparison to those given in Table 2. The values of the occupational parameters P_2 and P_3 are not significantly different at -0.006 and -0.062, respectively. These weak second-order reflections are also discussed in the next section.

* A list of observed and calculated structure factors has been deposited with the British Library Document Supply Centre as Supplementary Publication No. SUP 71029 (3 pp.). Copies may be obtained through The Technical Editor, International Union of Crystallography, 5 Abbey Square, Chester CH1 2HU, England.

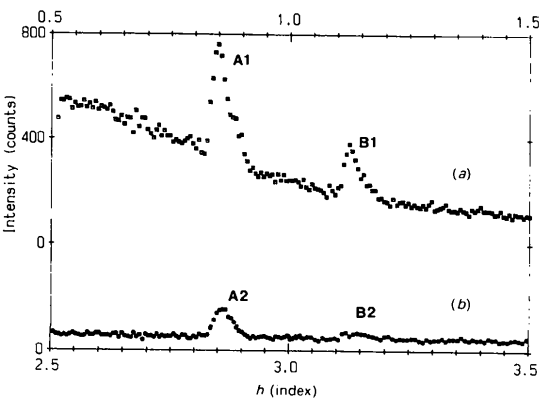

Fig. 4. Changes of intensity difference for pairs of first-order satellites. (*a*) The pair *A*1 ($000\bar{1}$ or $0.86\ \bar{0.43}\ 0$) and *B*1 ($2\bar{1}0\bar{1}1$ or $1.14\ \bar{0.57}0$), (*b*) the pair *A*2 ($2\bar{1}01\bar{1}$ or $2.86\ \bar{1.43}\ 0$) and *B*2 ($4\bar{2}0\bar{1}1$ or $3.14\ \bar{1.57}\ 0$). The upper scale corresponds to (*a*) and the lower scale to (*b*) using the basic reflection index h. The intensity scale is common to both pairs. Mo $K\alpha$ radiation, 40 kV × 30 mA, counting time 100 s for each point. The abrupt decrease in the background intensity for (*a*) is due to the air scattering where the 2θ starts at an angle as small as 7.6°.

Table 2. *Positional* (U_1–U_4), *occupational* (P_0–P_3) *and thermal parameters* (B_0–B_3) *for* Cu–Sb *compared to the previous study of* Au–Cd

	Cu–Sb	Au–Cd†
U_1	−0.0036 (9)	0.0025 (11)
U_2	−0.0062 (5)	0.0005 (8)
U_3	−0.0023 (1)*	
U_4	0.0030 (1)*	
P_0	0.805 (fixed)	0.667 (fixed)
P_1	0.115 (6)	−0.22 (4)
P_2	−0.013 (2)*	
P_3	−0.062 (3)*	
B_0	1.41 (5)	1.27 (8)
B_1	0.81 (6)	0.30 (7)
B_2	0.17 (4)*	
B_3	0.74 (5)*	

* Determined by using only nine second-order reflections. See also in the text.

† Determined by Yamamoto (1983).

Table 3. *Comparison of calculated* ($|F_{c_1}|$, $|F_{c_2}|$) *and observed structure factors* ($|F_o|$).

$|F_{c_1}|$ corresponds to the Onozuka model and $|F_{c_2}|$ to the present analysis, where reflection indices are expressed in three ways: indices of *hkl* are referred to the basic lattice, *HKL* to the Onozuka model and $h_1h_2h_3h_4h_5$ to the five-dimensional description of the present investigation. The five groups in the table from top to bottom correspond to reflections of basic, first-order, second-order $\mathbf{k}_1 + \mathbf{k}_2$ type, second-order $2\mathbf{k}_1$ or $2\mathbf{k}_2$ type and the values of the Onozuka model, respectively (× 4).

h	*k*	*l*	*H*	*K*	*L*	h_1	h_2	h_3	h_4	h_5	$\|F_{c_1}\|$	$\|F_{c_2}\|$	$\|F_o\|$
1	0	0	24	24	0	1	0	0	0	0	99	100	98
2	−1	0	72	0	0	2	−1	0	0	0	140	138	114
1	0	1	24	24	1	1	0	1	0	0	161	162	149
0.57	−0.14	0	17	7	0	1	−1	0	0	1	10	0	3
0.86	−0.43	0	31	0	0	0	0	0	1	−1	19	12	14
1.14	−0.57	0	41	0	0	2	−1	0	−1	1	17	7	11
1.43	−0.57	0	48	7	0	1	−1	0	1	0	8	13	12
0.57	−0.14	1	17	7	1	1	−1	1	0	1	16	10	15
1.43	−0.57	1	48	7	1	1	−1	1	1	0	13	7	8
0.29	0	0	7	7	0	−1	0	0	2	−1	4	1	0
0.71	0.	0	17	17	0	2	0	0	−2	1	3	2	3
1	−0.29	0	31	10	0	1	1	0	−1	−1	7	1	3
1.29	−0.29	0	38	17	0	0	1	0	1	−2	3	3	3
1.71	−0.71	0	58	7	0	3	−2	0	−1	2	3	1	0
0.29	0	1	7	7	1	−1	0	1	2	−1	6	4	4
0.71	0	1	17	17	1	2	0	1	−2	1	6	0	0
1	−0.29	1	31	10	1	1	1	1	−1	−1	0	1	2
1.29	−0.29	1	38	17	1	0	1	1	1	−2	5	0	0
0.28	−0.14	0	10	0	0	2	−1	0	−2	2	4	0	0
0.85	−0.15	0	24	13	0	0	−1	0	2	0	1	0	0
1.14	−0.28	0	34	14	0	2	−2	0	0	2	3	0	0
1.72	−0.86	0	62	0	0	0	0	0	2	−2	3	0	0
0.85	−0.15	1	24	13	1	0	−1	1	2	0	2	0	0
1.14	−0.28	1	34	14	1	2	−2	1	0	2	3	0	0
0.58	0	0	14	14	0						2	0	0
0.30	−0.15	0	11	0	0						3	0	0
0.42	0	0	10	10	0						4	0	0
0.58	−0.29	0	21	0	0						3	0	0
0.58	0	1	14	14	1						3	0	0
1	−0.42	1	34	4	1						3	0	0

Discussion

The final structure obtained by calculation of the parameters given in Table 2 is highly disordered. This was suspected from the weakness of the intensities of higher-order satellites and it is difficult to imagine a clear and definite structure model, or the incommensuration of the period.

Comparison with high-resolution electron microscopy studies

Onozuka *et al.* (1989) proposed a structural model for the same alloy, having the period of $M = 7.2$, by using high-resolution electron microscopy. The model is based on the superstructure of the ordered lattice [$7a_0$-$2H$-type structure according to Hirabayashi *et al.* (1970)]. The space lattice is trigonal with lattice parameters $a = 113.8$ and $c = 4.322$ Å. The space group is $P3c1$ and there are 2796 Cu and 660 Sb atoms in the unit cell. The structure calculation is tedious: there are 227 Cu and 49 Sb atoms at 12(g) sites having independent x and y parameters, and 12 Cu and 12 Sb atoms at 6(f) sites having independent y parameters and there are 576 independent coordination parameters in all. These parameters are taken from the Onozuka model. Since no information was available about the temperature factors they were assumed to be isotropic and identical, $B_{iso} = B_{Cu} = B_{Sb} = 1.0$ Å^2, which is the averaged value for Cu and Sb given in *International Tables for X-ray Crystallography* (1962, Vol. III, pp. 234, 239). We do not consider the uncertainty of the temperature factors to be serious because the comparison with the Onozuka model was restricted to the nearest neighbour of the reciprocal lattice origin. In this unit cell, 100 and $2\bar{1}0$ reflections of the basic lattice are described as 24240 and 7200, respectively. The incommensuration of the period can be avoided by considering the giant cell. The structure factors calculated with the Onozuka model are compared with those of the present analysis and with those observed in Table 3. Since our analysis is based on modulation waves up to second order, the bottom group of the reflections does not correspond to any of the present reflections $h_1h_2h_3h_4h_5$. The agreement factors are $R = 0.29$ for the Onozuka model and $R = 0.14$ for the present model. The intensity profiles for the two reflections that are expected to be observed from the Onozuka model (see Table 3) are shown in Fig. 5, indicating the absence of diffraction peaks.

Comparison with the Au–Cd *alloy*

For simplicity, we approximate the period M of the present Cu–Sb alloy to be 7 instead of 7.19, in order to facilitate a direct comparison with the previous study of Au–Cd (Watanabe & Iwasaki, 1982; Yamamoto, 1983). The concentration distribution for Cu atoms can be calculated from the values of P_0, P_1, P_2 and P_3. The displacement-modulation parameters of U_1 and U_2 are taken into account and final results for each component are indicated in Fig. 6. The positions of maximum Sb concentration, indicated by triangles, are paired, while in the case of Au–Cd, the corresponding maxima of Cd are in isolated positions (see Fig. 4 of Watanabe & Iwasaki,

1982). It is remarkable that the first-order component, P_1, has an opposite sign to that of Au–Cd (see Table 2). This difference in the sign seems to arise from the concentration value, P_0. In the case of Au–Cd, P_1 represents the perfect Cd site, while in Cu–Sb, P_1 represents the perfect Cu site, but not the Sb site. This is because the low concentration of Sb makes it difficult to attain the perfect Sb site by only first- or second-order modulation waves.

We now examine the displacement waves and their relation to concentration waves. In the Au–Cd alloy, the atomic displacements are mainly longitudinal and the contribution of the transverse component is negligibly small. This can be adequately explained if we assume that the charge-density wave (CDW) is associated with the concentration-wave maxima of cadmium, as described in the paper of Watanabe & Iwasaki (1982). In the case of the present Cu–Sb alloy, the amplitude of the transverse wave is larger than that of the longitudinal wave. Since the longitudinal component involves attraction along the direction connecting two nearest-neighbour atoms, the transverse component is preferable in the Cu–Sb alloy which forms dimers (triangles in Fig. 6*a*) in a close-packed plane normal to the *c* axis. This is a result of a larger atomic size difference between Cu and Sb in comparison with that between Au and Cd. The maximum atomic displacement for Cu–Sb is 0.023 Å (at the corners of the parallelogram in Fig. 6), which is about three times larger than that of the Au–Cd alloy.

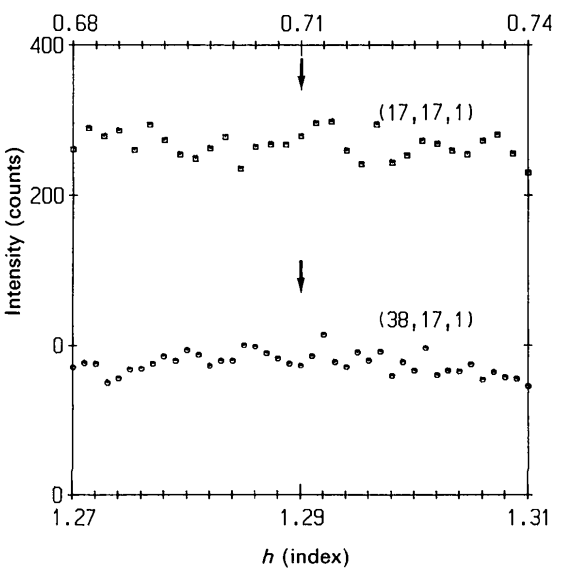

Fig. 5. Profiles of the satellite positions expected from the Onozuka model. The 17171 or 0.7101 reflection corresponds to the upper scale and the 38171 or $1.29\overline{0.29}1$ to the lower scale, where the horizontal axis is given in terms of the basic reflection index *h*. The arrows indicate the peak positions expected from the Onozuka model. The vertical scale is common to both. See also Table 3. Cu $K\alpha$ radiation, 40 kV × 30 mA, counting time 200 s for each point.

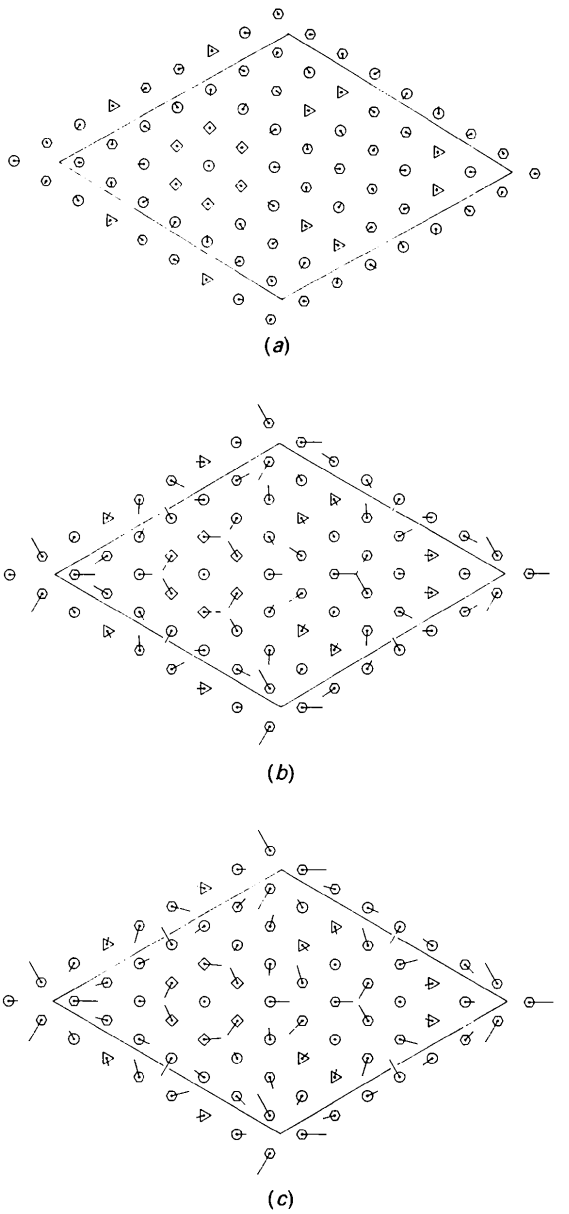

Fig. 6. Distribution of the occupancies of Cu atoms and directions of displacements in the ε-phase for an atomic plane normal to the *c* axis. The occupational probability of Cu atoms is represented by four symbols: circles, hexagons, squares and triangles correspond to >0.9, 0.9–0.7, 0.7–0.6 and <0.6, respectively. The black dots in each symbol indicate the basic lattice points and solid lines attached to dots indicate the atomic displacements which are enlarged by a factor of about 80. (*a*) The longitudinal component. (*b*) The transverse component. (*c*) Total displacement. The atomic displacements are calculated with first-order modulation only.

The authors wish to express their gratitude to Professor H. Iwasaki, Institute of High Energy Physics, and Professor T. Sakurai, Institute for Materials Research, Tohoku University, for their continuous encouragement throughout the present investigation. Dr Yamamoto, National Institute for Research in Inorganic Materials, has kindly permitted the authors to use his program *REMOS* for the present study.

References

BUDKOWSKI, A., MARINKOVIC, V., PRODAN, A. & BOSWELL, F. W. (1990). *Phys. Status Solidi A*, **117**, 351–362.
GUNZEL, E. & SCHUBERT, K. (1958). *Z. Metallkd.* **49**, 124–133.
HANSEN, M. (1958). *Constitution of Binary Alloys*, pp. 622–628. New York: McGraw-Hill.
HIRABAYASHI, M., HIRAGA, K. & SHINDO, D. (1981). *J. Appl. Cryst.* **14**, 169–177.
HIRABAYASHI, M., YAMAGUCHI, S., HIRAGA, K., INO, N., SATO H. & TOTH, R. S. (1970). *J. Phys. Chem. Solids*, **31**, 77–94.
JANNER, A., JANSSEN, T. & DE WOLFF, P. M. (1983). *Acta Cryst.* A**39**, 658–666.
JANSSEN, T. & JANNER, A. (1987). *Adv. Phys.* **36**, 519–624.
KATAOKA, M. & IWASAKI, H. (1981). *J. Phys. F*, **11**, 1545–1556.
OKAMURA, K., IWASAKI, H. & OGAWA, S. (1968). *J. Phys. Soc. Jpn*, **24**, 569–579.
ONOZUKA, T., KAKEHASHI, S., TAKAHASHI, T. & HIRABAYASHI, M. (1989). *J. Appl. Cryst.* **22**, 272–282.
STEURER, W. (1989). *Phase Transit.* **16–17**, 103–118.
WATANABE, Y. & IWASAKI, H. (1982). *J. Appl. Cryst.* **15**, 174–181.
YAMAGUCHI, S. & HIRABAYASHI, M. (1972). *J. Phys. Soc. Jpn*, **33**, 708–716.
YAMAMOTO, A. (1983). *Acta Cryst.* B**39**, 17–20.

Acta Cryst. (1993). B**49**, 661–675

The Structure of Decagonal $Al_{70}Ni_{15}Co_{15}$

BY W. STEURER, T. HAIBACH AND B. ZHANG

Institut für Mineralogie der Universität, Welfengarten 1, *D*-3000 *Hannover* 1, *Germany*

S. KEK

Fachrichtung Kristallographie, Universität des Saarlands, D-6600 *Saarbrücken* 11, *Germany*

AND R. LÜCK

Institut für Werkstoffwissenschaft, MPI für Metallforschung, Seestrasse 75, *D*-7000 *Stuttgart* 1, *Germany*

(*Received* 11 *December* 1992; *accepted* 25 *March* 1993)

Abstract

The quasiperiodic structure of decagonal $Al_{70}Ni_{15}Co_{15}$ was determined on the basis of X-ray single-crystal intensity data using the *n*-dimensional embedding method. Centrosymmetric five-dimensional space group $P10_5/mmc$, three-dimensional reciprocal and direct quasilattice parameters: $a_i^* = 0.2636\ (1)\ Å^{-1}$, $i = 1,\ldots, 4$, $a_5^* = 0.24506\ (3)\ Å^{-1}$, $a_i = 3.794\ (1)\ Å$, $i = 1,\ldots, 4$, $a_5 = 4.0807\ (3)\ Å$. Five-dimensional unit-cell parameters: $d_i = 3.393\ (1)$, $d_5 = 4.0807\ (3)\ Å$, $\alpha_{ij} = 60°$, $\alpha_{i5} = 90°$, $i, j = 1,\ldots, 4$, $V = 302.4\ Å^5$, $M_r = 36.54$, $D_x = 4.5\ Mg\ m^{-3}$, $\mu = 10.1\ mm^{-1}$, Mo $K\alpha$, $wR = 0.078$, $R = 0.091$ for 253 unique reflections and 21 variables. A five-dimensional structure model was obtained by Patterson syntheses and refined by the least-squares technique. High-resolution electron-density maps were calculated by the maximum-entropy method. The structure is formally built up by two quasiperiodic atomic layers with stacking sequence *Aa* (*a* denotes the layer *A* rotated around $2\pi/10$). It is essentially isotypic to that of decagonal $Al_{65}Cu_{20}Co_{15}$ and shows locally a close resemblance to monoclinic $Al_{13}Co_4$. Columnar clusters parallel to the local tenfold screw axes, formed by ten pentagonal antiprismatic columns surrounding a central column, are found to be the basic structural building elements. Quasiperiodicity is forced by the formation of interconnected networks of closed icosagonal rings of pentagonal and rectangular structure motifs.

Introduction

Decagonal quasicrystals represent interesting intermediate states between icosahedral and crystalline phases with anisotropic physical and mechanical properties. The stable decagonal phase $Al_{70}Ni_{15}Co_{15}$, with needle-like decagonal prismatic morphology, was first synthesized by Tsai, Inoue & Masumoto (1989) by slow solidification. Its stability range between 773 K and the melting point was studied by Kek (1991). Other stable decagonal phases were found in the systems Al–Cu–Co by He,